

J. Kengne¹, J.C. Chedjou¹, K. Kyamakya²

University of Dschang (Cameroon) (1), University of Klagenfurt (Austria) (2)

Stability and Bifurcation Analysis of Electronic Oscillators: Theory and some Experiments

Abstract. We consider the electronic structure of a shunt-fed Colpitts oscillator. This oscillator is a feedback circuit built with a single bipolar junction transistor which is responsible of the nonlinear behavior of the complete circuit. The interest of investigating the dynamics of this circuit is justified by its multiple potential applications in the field of engineering and also by the striking/tremendous and very complex behavior the oscillator can exhibit, leading to periodic, multi-periodic and chaotic motions. We discuss some potential applications of the shunt-fed Colpitts oscillator. The modeling process leads to the derivation of mathematical equations (ODEs) to describe the behavior of the shunt-fed Colpitts oscillator. Using these equations, the stability and bifurcation analyzes are carried out and basins of attraction of stable solutions are obtained as well as some bifurcation diagrams showing the extreme sensitivity of the system to tiny changes in the values of the electronic circuit components. Analytical, numerical and experimental methods/approaches are considered to get full insight of the dynamical behavior of the proposed oscillator. Analytical and numerical results are validated by the results obtained from a real physical implementation (Hardware implementation) of the oscillator.

Keywords. Shunt-fed Colpitts oscillator, Loop gain, Modeling, Stability, Bifurcation, Chaos

1 Introduction

During the last decades, a tremendous attention has been devoted to the analysis of the nonlinear behavior of sinusoidal oscillators [1-18]. The focus on this analysis is explained by the rich and complex behavior nonlinear oscillators can exhibit and also the various potential technological applications of such oscillators. Indeed, in their nonlinear states these oscillators can be exploited in many applications. In their regular states, the oscillators can be used for instrumentations and measurements, while the chaotic behavior (irregular state) exhibited by the oscillators can be used in securing communications and/or for random waves generation as well, just to name a few. Another interesting potential application of nonlinear oscillators can be related to finding solution to various problems in plasma physics, such as designing both microwave and transformer devices [17-18]. These applications are classically realized by one-stage bipolar junction transistor oscillators, the nonlinearity in these oscillators being a direct consequence of the nonlinear character of the transistor. Such applications require highly stable oscillators with large frequency bandwidths. Further, these oscillators must be robust to noise at high frequencies.

The drive towards increasingly higher operating frequencies (by means of single-transistor LC oscillators) for communication products is advantageous as it provides to circuit designers the possibility of integrating as much as possible such oscillators on a single chip (i.e. integrated circuit).

Concerning the nonlinear dynamics of single-transistor LC oscillators, some interesting works have been carried out. Reference [1] develops a methodological approach to the analysis and design of a Colpitts oscillator. A nonlinear approach for the two quasi-sinusoidal and chaotic operation modes is considered; in particular the generation technique of regular and irregular (chaotic) oscillations in terms of the circuit parameters is shown. Reference [2] exploits a Lur'e model to demonstrate the occurrence of chaos in the Colpitts oscillator. Components of the autonomous chaotic Colpitts oscillator causing the instability of equilibrium points are identified. The study in [2] is extended (by the same authors see [3]) to the case of a forced (non-autonomous) Colpitts oscillator. Both amplitude and frequency of the external excitation are used for chaos control within the oscillator. The dynamic- maps of phase locking transitions are depicted by measurements. Both simulation and experimental results showing the exhibition (by the oscillator) of the injection-locked dynamics are presented. Reference [4] considers the investigation of the nonlinear dynamical

behavior of two different self-driven oscillators leading to chaotic dynamics. A piecewise-linear model (PWL) is derived to describe the dynamics of a transformer coupled oscillator and, various bifurcation diagrams are obtained to illustrate some striking scenarios leading to chaos. By exploiting a feedback model of such a system, the loop gain of the oscillator is derived and its strong dependence with the nonlinear dynamics of the oscillator is demonstrated. Both Pspice based simulation and laboratory experiment (real physical implementation) are performed to confirm the numerical results.

This paper considers a shunt-fed structure of the Colpitts oscillator. The advantage of such a structure (amongst many others) can be found in the practical realization. Indeed, this structure is simple to realise. Further, the good stability of the fundamental characteristics (i.e. amplitude and frequency) of the waveforms generated by such a structure is due to the fact that the biasing current is not flowing through the oscillatory network as observed in the series-fed structure. Another advantage of the shunt-fed Colpitts oscillator is the possibility of deriving corresponding equations from which can be shown the capability of the oscillator to perform in a large frequency bandwidth, ranging from low frequencies (e.g. the order of Hertz) to high frequencies (e.g. the order of gigahertz). This could be achieved by performing an appropriate time scaling of the equations which are derived to describe the nonlinear dynamical behavior of the oscillator. Another interesting feature of this oscillator is the intrinsic nonlinear character of its analog device (e.g. the current-voltage characteristics of the bipolar junction transistor is exponential); this character can easily give rise to regular (periodic) oscillations or chaotic dynamics depending upon a suitable choice of the system parameters.

We consider the shunt structure of the Colpitts oscillator in Fig.1. This particular structure was recently introduced in reference [5]. In this reference we used a fourth-order nonlinear equation to investigate the bifurcation structures exhibited by the shunt Colpitts oscillator. Using one of the feedback divider capacitors as control parameter, various bifurcation diagrams were obtained showing the richness of modes exhibited by the oscillator and some scenarios leading to chaos. Both Pspice based simulations and laboratory experimental measurements were performed to validate the results of the modeling process. Nevertheless, an improvement of these results was found necessary to facilitate both the design and implementation processes and increase the performance of the oscillator as well. This work addresses these issues. Some key problems investigated

could be reducing both the number of parameters involved and the state space dimension as well. It is worth noticing that such an approach is of great importance both for analysis and design purposes.

Our aim in this paper is to contribute to the general understanding of the nonlinear dynamical behavior of the shunt-fed Colpitts oscillator and complete the results obtained so far by (a) carrying out a systematic and methodological analysis of the dynamical behavior of the oscillator; (b) providing both theoretical and experimental tools which will be of precious use for the design and control purposes as they could provide full insight of/on the nonlinear dynamical behavior of the oscillator; (c) pointing out some of the unknown and striking behavior of the shunt-fed Colpitts oscillator.

The rest of the paper is organized as follows. In section 2 we use a simplified equivalent model of the bipolar junction transistor for the modeling process. The state equations of the circuit designed (i.e. the shunt Colpitts oscillator) are obtained. Section 3 investigates the stability of fixed points. The analysis of local bifurcations of fixed points is considered. Different types of bifurcations likely to occur are found. Conditions for the occurrence of Hopf bifurcations are derived. Section 4 deals with numerical simulation. Various bifurcation diagrams associated to their corresponding graphs of largest one-dimensional (1D) numerical Lyapunov exponents are obtained showing both complex and striking scenarios to chaos. Section 5 is concerned with the experimental study. The design and real physical implementation of the oscillator are considered using electronic components. Experimental results are compared with both analytical and numerical results and a very good agreement is obtained. Section 6 deals with conclusions and proposals for further works.

2 Mathematical modeling of the shunt-fed Colpitts Oscillator

2.1 Circuit description

Figs. (1) show the electronic structure proposed for the shunt-fed Colpitts oscillator. Fig. (1a) is the complete circuit of the oscillator while Fig. (1b) is a simplified model of the bipolar junction transistor used in the modeling process.

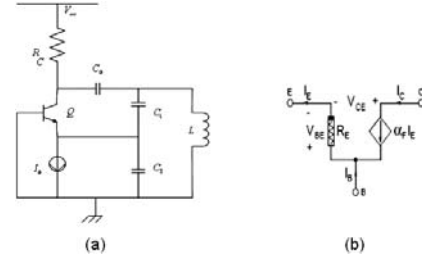
The bipolar junction transistor Q , used in the common-base configuration, plays the role of nonlinear gain element. The resonant network uses split capacitance and is an identification feature of the Colpitts oscillator. The coupling capacitor C_3 is supposed to have very low impedance at the operating/running frequencies. The bias is provided by the DC voltage source V_{CC} and the current source I_0 . The

resistor R is used to set the equilibrium point of the circuit. The main difference between the series-fed and the shunt-fed Colpitts oscillators is the bias current which doesn't flow through the tank coil when dealing with the fed-shunt Colpitts. This situation justifies the name "shunt-fed". This shunt when performed keeps a high circuit's quality factor, and results in better frequency stability.

The resonant frequency of the unloaded tank circuit, which is an estimator of the fundamental frequency of the oscillator, is given by:

$$(1) \quad f_0 = \frac{1}{2\pi} \sqrt{\frac{C_1 + C_2}{LC_1 C_2}}$$

In this oscillator, the only nonlinear component (necessary for setting up chaotic oscillations) is the bipolar junction transistor (BJT). The rest of circuit components are assumed linear.



Figs.1: (a) Circuit diagram of the shunt-fed Colpitts oscillator and (b) the BJT model consisting of one current-controlled source and a single diode.

2.2 State equations

According to the qualitative theory in nonlinear dynamics, we select a minimal model [18] for the circuit. The idea is to consider as simple a circuit model as possible which maintains the essential feature exhibited by the real oscillator. To carry out our modelling process, the following simplifying hypotheses are considered:

- Ideal bias source, i.e., the bias current in the emitter of the bipolar junction transistor is provided by an ideal current source I_0 .

- Passive and reactive elements are assumed ideal.

- The bipolar junction transistor is modeled simply by a (voltage-control) nonlinear resistor R_E and a linear current source (see Fig.1a).

- The current-voltage (V-I) characteristic of R_E is modeled by an exponential function, namely

$$I_E = f(V_{BE}) = I_S \left(\exp\left(\frac{V_{BE}}{V_T}\right) - 1 \right) \approx I_S \exp\left(\frac{V_{BE}}{V_T}\right)$$

for $V_{BE} > V_T$; where I_S is the inverse saturation

(2) current and $V_T \approx 26mV$ at room temperature.

- The common-base forward short-circuits current gain α_F is approximately equal to unity ($\alpha_F \approx 1$). This corresponds to neglecting the base current.

- Parasitic effects are neglected (e.g. in C_{ce} and C_{be}). In case these effects are considered, they will be added in parallel with C_1 and C_2 respectively.

We emphasize that the assumptions above do not alter the qualitative dynamics of the system (i.e. they do not add extra dynamics to the system) and we suppose that only the quantitative dynamics (e.g. position of the attractors in the parameter space) can be affected as discussed in [1].

We use the electrical circuit theory and some assumptions to derive the following model of the shunt oscillator:

$$(3a) \quad RC_1 \frac{dV_{C_1}}{dt} = V_{cc} - V_{C_1} - V_{C_2} - V_{C_0} - R\alpha_F I_E - R I_L$$

(3b)

$$RC_2 \frac{dV_{C_2}}{dt} = V_{cc} - V_{C_1} - V_{C_2} - V_{C_0} + R((1-\alpha_F)I_E - I_L - I_0)$$

(3c)

$$L \frac{dI_L}{dt} = V_{C_1} + V_{C_2}$$

Eqs. (3) describe the dynamics of the shunt-fed oscillator.

I_L denotes the current flowing through the inductor;

$V_i (i = 0, 1, 2)$ stand for the voltages across capacitors

C_i . For the sake of simplicity, it can be obtained from Eqs. (3) the following normalized sets of ordinary differential equations (Eqs. (4)) to describe the dynamical behavior of the shunt-fed Colpitts oscillator:

$$(4a) \quad \frac{dx_1}{dt} = -Qk(x_1 + x_2) - \frac{g}{Q(1-k)}[x_3 + n(x_2)]$$

$$(4b) \quad \frac{dx_2}{dt} = -Qk(x_1 + x_2) - \frac{g}{Qk}x_3$$

$$(4c) \quad \frac{dx_3}{dt} = \frac{Qk(1-k)}{g}(x_1 + x_2)$$

$$(4d) \quad n(x_2) = \exp(-x_2) - 1$$

$$(4e) \quad k = \frac{C_2}{C_1 + C_2}, \quad Q = \frac{L\omega_0}{R}, \quad \text{and}$$

$$g = \frac{LI_0}{V_T R(C_1 + C_2)}$$

x_1 and x_2 are normalized voltages across capacitors C_1 and C_2 and x_3 represents the normalized current flowing in the inductor L .

Notice the remarkable simplicity of the nonlinear term in the proposed model. Indeed, only the first equation (Eq. (4a)) contains a nonlinear term. It can be shown by means of some mathematical algebraic manipulations that Eqs. (4) are equivalent to the following Jerk model:

$$(5) \quad \frac{d^3x_2}{dt^3} + Q\frac{d^2x_2}{dt^2} + [1 + g(1 + n(x_2))] \frac{dx_2}{dt} - \frac{g}{Q}n(x_2) = 0$$

Further, the following equilibrium point can be derived from the preceding equations describing the nonlinear dynamics of the shunt Colpitts oscillator:

$$(6) \quad (\bar{V}_1 \quad \bar{V}_2 \quad \bar{i}_L)^T = (V_T \ln(I_0/I_S) \quad -V_T \ln(I_0/I_S) \quad 0)^T$$

As it appears in Eq. (5), the proposed structure of the shunt Colpitts oscillator is modeled by a third order nonlinear ordinary differential equation which is very sensitive to the parameters g and Q . Another interesting remark is related to the parameter k which does not significantly affect the behavior of the Shunt Colpitts oscillator. In fact, the parameter k acts like a scaling factor/coefficient for the attractors exhibited by the shunt Colpitts oscillator. It should be worth noticing that the parameters g and Q can lead to a precise physical interpretation in case the issue is related to the design of an ideal/optimal structure of the Colpitts oscillator. Specifically, the quality factor Q measures the selectivity of the resonant circuit, while g admits a precise physical meaning in the context of Barkhausen criterion related to the series-fed Colpitts oscillator [1] which defines the oscillator condition according to classical linear analysis.

3. Stability analysis

The stability analysis is carried out by transforming Eqs. (4) in the form of Eq. (7).

$$(7) \quad \frac{dV}{dt} = F(V, \mu)$$

Where $V = (x_1, x_2, x_3)$ is an autonomous vector field and $\mu = F(k, Q, g)$ is an element of the parameter space. Eq. (7) generates a flow $\phi = \{\phi^T\}$ on the phase space $R^3 \times S^1$ and there exist a global map: $P: \Sigma_C \rightarrow \Sigma_C$

$$V_p(x_1, x_2, x_3) \rightarrow P(V_p) = \{\phi^T\}_{\Sigma_C(x_1, x_2, x_3)}$$

where (x_1, x_2, x_3) represents the coordinates of the projection of the attractors onto the Poincaré cross section Σ_C defined by $\Sigma_C = \{(x_1, x_2, x_3) \in R^3 \times S^1\}$. The perturbation analysis [17-18] is used to investigate the stability of oscillatory solutions in the Poincaré map Σ_C . Thus, Eq. (4) is perturbed by adding a small perturbation $\delta V_P = (\delta x_1, \delta x_2, \delta x_3)$ to the steady state $V_{PO}(x_{10}, x_{20}, x_{30})$. The variational differential equation (Eq. (8a)) is derived with the corresponding variational matrix defined in Eq. (8b).

$$(8a) \quad \frac{d\delta V_P}{dt} = DF(V_{PO})\delta V_P$$

$$(8b) \quad DF(V_{PO}) = \begin{bmatrix} -Qk & -Qk + \frac{g \exp(-x_{20})}{Q(1-k)} & \frac{-g}{Q(1-k)} \\ -Q(1-k) & -Q(1-k) & \frac{-g}{Qk} \\ \frac{Qk(1-k)}{g} & \frac{Qk(1-k)}{g} & 0 \end{bmatrix}$$

The stability of periodic motion is obtained according to the real parts of the roots of the following characteristic equation ($\det[DF(V_{PO}) - \lambda I_d] = 0$):

$$(9) \quad \lambda^3 + Q\lambda^2 + (1+g)\lambda + \frac{g}{Q} = 0,$$

obtained by considering very small amplitudes of the steady states. Therefore the states of the oscillator (e.g. stable or unstable states, Hopf bifurcation, and subcritical bifurcation, etc...) are obtained by the roots (i.e. eigenvalues solutions) of Eq. (9).

4 Results

4.1 Analytical results

We investigate analytically the stability of fixed points and the stability of oscillatory states in the weakly nonlinear response. Fig. 2 shows in the complex plane $(\text{Re}(\lambda), \text{Im}(\lambda))$ the representation of the eigenvalues (roots of the characteristic equation). These roots are obtained (using the Newton-Raphson algorithm) for

$Q \in [0.1, 0.8]$ and $g \in [0.25, 5]$. From Fig. 2 one can have an idea on both the stability of periodic solutions and the different types of bifurcation likely to appear in the system. Since $DF(V_{PO})$ is a real matrix, complex eigenvalues in complex conjugate pairs are responsible of the observed symmetry along the real axis. Thus if the real parts of the eigenvalues (λ) are all negative, the rate is of the contraction type or otherwise of the expansion. If the eigenvalues are all real, the contraction or the expansion is observed near the steady state while the complex values of the eigenvalues show the contraction or expansion of the spiral. If there exist eigenvalues having real parts with different sign, the equilibrium state is called saddle; an equilibrium point whose eigenvalues have nonzero real parts is called hyperbolic. On the other hand period doubling bifurcation is observed if there exists an eigenvalue ($\lambda = -1$) while bifurcations of the Hopf type are observed if the following conditions are satisfied: (a) there exists a pair of pure imaginary complex eigenvalues ($\lambda_{1,2} = \pm j\Im m(x)$;

(b) $\left(\frac{d\lambda}{d\alpha}\right)_{\alpha=\alpha_c} \neq 0$ (non zero crossing speed), α being

the bifurcation control parameter. α_c is the critical value for the occurrence of Hopf bifurcation, obtained from the equation $\Re e(\lambda) = 0$.

Considering the previous results it clearly appears that our system for the given parameters g and Q can undergo various types of bifurcations namely: saddle bifurcation, period-doubling bifurcation and Hopf bifurcation. We have derived the following relationships between the parameters of the model (describing the dynamics the oscillator) for the occurrence of Hopf bifurcation:

$$(10a) \quad \omega_{osc}^2 = \frac{\omega_0^2}{1-Q^2}$$

$$(10b) \quad \frac{g(1-Q^2)}{Q^2} = 1$$

By constructing the Routh-array of the oscillator it can be shown that the equilibrium point of the system is stable if the following conditions are satisfied:

$$(11a) \quad \frac{g(1-Q^2)}{Q^2} < 1 \quad Q \in]0, 1[$$

Or

$$(11b) \quad Q > 1 \quad (\text{The equilibrium point is always stable})$$

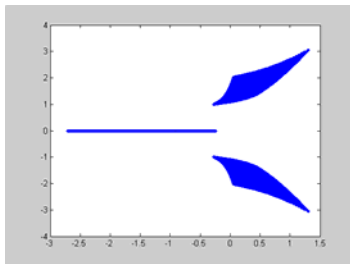


Fig.2: Representation of the eigenvalues solutions in the complex

plane.

4.2 Numerical results

Eqs. (4) are solved numerically to define routes to chaos. We use the four-order Runge-Kutta algorithm for the sets of parameters used in this work, the time step is always $\Delta t = 0.005$ and the calculations are performed using real variables and constants in extended mode. The integration time is always $T \geq 10^6$. Here the types of motion are identified using two indicators. The first indicator is the bifurcation diagram, the second being the largest 1D numerical Lyapunov exponent denoted by

$$(12a) \quad \lambda_{max} = \lim_{t \rightarrow \infty} \left[\frac{1}{t} \ln(d(t)) \right]$$

where

$$(12b) \quad d(t) = \sqrt{(\delta x_1)^2 + (\delta x_2)^2 + (\delta x_3)^2}$$

and computed from the variational equations obtained by perturbing the solutions of Eqs. (5) as follows: $x_1 \rightarrow x_1 + \delta x_1$, $x_2 \rightarrow x_2 + \delta x_2$, and $x_3 \rightarrow x_3 + \delta x_3$.

$d(t)$ is the distance between neighbouring trajectories [5]. Asymptotically, $d(t) = \exp(\lambda_{max} t)$. Thus, if $\lambda_{max} > 0$, neighboring trajectories diverge and the state of the oscillator is chaotic. For $\lambda_{max} < 0$, these trajectories converge and the state of the oscillator is non-chaotic. $\lambda_{max} = 0$ for torus states of the oscillator.

In the preceding section, we have shown that the dynamics of the oscillator is governed only by the couple of parameters Q and g , the third parameter k being a scaling factor with no significant effect on the system's attractor. Setting the value of $Q = 0.1718$ and $k = 0.67$, we analyze the effects of the control parameter g on the behavior of the system. The scanning process is performed to investigate the sensitivity of the oscillator to tiny changes in g . The use of g as the control parameter revealed the richness and the variability of the bifurcation modes in the Colpitts oscillator within its nonlinear regime. The extreme sensitivity of the oscillator to tiny changes in g is observed. Regions of non oscillations, regions of divergence solutions and regions of oscillations are obtained by monitoring g . In the latter case, various types of oscillations are obtained: periodic, quasi-periodic and chaotic oscillations. Such oscillations are due to the presence of the nonlinearity in the Colpitts oscillator. Fig. 3 presents a bifurcation diagram showing a transition to chaos through period-doubling scenarios. It is also shown the extreme sensitivity of the oscillator to tiny changes in g . Windows of chaotic dynamics alternate with tiny windows of regular dynamics.

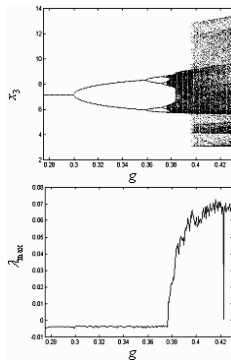


Fig. 3: Bifurcation diagram of the shunt-fed Colpitts oscillator and the graph of 1D largest numerical Lyapunov exponent.

The positive value of λ_{\max} is a signature of chaos.

4.3 Experimental results

This section provides sample results to validate the analytical and numerical results. Using the same values of the system parameters we determine the corresponding electronic coefficients to design and implement the electronic circuit of Fig. 4. This figure is the design of the experimental setup for the implementation of the shunt-fed Colpitts oscillator built on a breadboard.

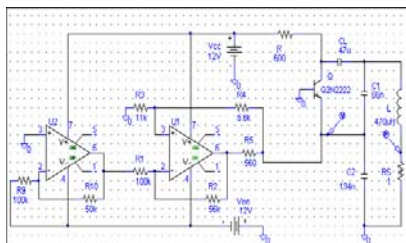


Fig.4: Experimental setup for the measurements on the shunt type Colpitts

The following values of circuit components are used which correspond to the same set of the parameters values used in the analytical and numerical methods: $C_1 = 66nF$, $C_2 = 134nF$, $C_3 = 22\mu F$, $L = 470\mu H$, and $V_{CC} = 12V$. The electronic network consisting of the operational amplifier U_1 is an implementation of the ideal current generator. U_2 is used in a voltage circuit inverter. A 1Ω resistor is added in series to the inductor L to sensor it's current i_L . The experimental results are obtained by observing the time evolution of the voltage across the capacitor C_2 and by plotting phase portraits (V_{C_2}, i_L) .

Experimental results were generally close to those obtained analytically and numerically. Basically, some bifurcations obtained analytically and numerically were observed experimentally. In Figs. 5 is shown some sample results of the comparison between numerical waveforms (a) and experimental waveforms (b), and the comparison between numerical phase portraits (c) and experimental phase portraits (d). Both qualitative and quantitative very good agreements were obtained between different methods.

5 Conclusion

This paper has dealt with the analysis of the shunt fed Colpitts oscillator. The analytical study of the oscillator has revealed various striking bifurcations. These bifurcations were confirmed analytically and experimentally.

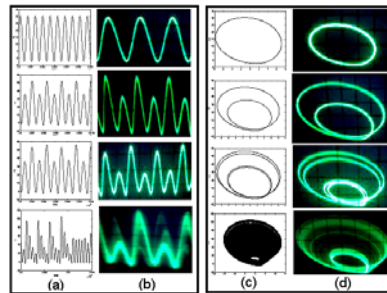


Fig.5: Qualitative comparison of experimental and numerical results: (a) and (b): numerical and experimental wave forms; (c) and (d) numerical and experimental phase portraits of the oscillator

REFERENCES

- [1] G. M. Maggio, O. De Feo and M. P. Kennedy, "Nonlinear analysis of the Colpitts oscillator and applications to design", IEEE Transaction on Circuits and Systems, CAS-46, pp.1118-1130, 1999.
- [2] J. C. Liu, H. C. Chou, and J. H. Chou, "Clarifying the chaotic phenomenon in an oscillator by Lur'e system form", Microwave and Opt. Tech. Letters, Vol. 22, pp. 323-328, 1999.
- [3] J. C. Liu, H. C. Chou, and J. H. Chou, "Non-autonomous chaotic analysis of the Colpitts oscillator with Lur'e system", Microwave and Opt. Tech. Letters, Vol. 36, pp.175-181, 2003.
- [4] J. Zhang, "Investigation of chaos and nonlinear dynamical behaviour in two different self-driven oscillators", Ph.D. thesis, University of London, 2001.
- [5] J. C. Chedjou, K. Kyamakya, Van Duc Nguyen, I. Moussa and J. Kengne "Performance evaluation of analog systems simulation methods for the analysis of nonlinear and chaotic modules in communications", ISAST Transactions on Electronics and Signal processing, N°1, vol.2, 2008, pp71-82.
- [6] G. A. Kriegsmann, "Bifurcation in classical bipolar transistor circuits", SIAM (Studies Applied Maths) Vol. 49, pp. 390-403, 1989.
- [7] M. Kennedy "Chaos in the Colpitts oscillator". IEEE Transaction on Circuits and Systems-1, vol.41, pp.771-774, 1994.
- [8] M. P. Kennedy, "On the relationship between chaotic Colpitts oscillator and Chua's circuit", IEEE Transaction on Circuits and Systems, CAS-42, pp.373-376, 1995.
- [9] G. M. Maggio, C. Kennedy, and M. P. Kennedy, "Experimental manifestations of chaos in the Colpitts oscillator", in Proc. ISSC'97, Derry, Ireland, June 1997, pp. 235-242.
- [10] J. Zhang, X. Chen and A. Davis. "High frequency chaotic oscillations in a transformer- coupled oscillator". Proc. of NDES'99, Ronne, Denmark, pp.213-216, 1999.
- [11] C. Wegene and M. Kennedy. " RF chaotic Colpitts oscillator". Proc. Of NDES'95, Dublin, Ireland, pp.255-258, 1995.
- [12] Y. Hosokawa, Y. Nishio and Akio Ushida, "RC-Transistor chaotic circuit using phase-shift oscillators", Proc. Int. Symp. On Nonlinear Theory and its application (Nolta'98), Vol.2(1998),603-606.
- [13] Nikolai F. Rulkov and Alexander R. Volkovskii, "Generation of broad-band chaos using blocking oscillator". IEEE Transaction on Circuits and Systems-1, vol.48, No.6, 2001.
- [14] A. Najumas and A. Tamasevicius. "Modified Wien-bridge oscillator for chaos". Electronics letter, 31, pp.335-336, 1995.
- [15] A. A. Andronov, A. A. Vitts, and S. E. Khaikin, "Theory of oscillations". New York, Pergammon, 1996.
- [16] L. O. Chua, C. W. Wu, A. Huang, and G. Q. Zhong, "A universal circuit for studying and generating chaos-Part I: Routes to chaos", IEEE Transaction on Circuits and Systems-1, vol.40, No.10, pp.731-744, 1993.
- [17] Chance M. Glenn, "Synthesis of a Fully-integrated Digital Signal Source for communication from Chaotic Dynamics-based Oscillations", Ph.D thesis, Johns Hopkins University, January 2003.
- [18] G. M. Maggio, O. De Feo and M. P. Kennedy "A general method to predict the amplitude of oscillations in nearly sinusoidal oscillators", IEEE Transactions on Circuits and Systems, Vol.51, August 2004, pp1586-1595.